Optical Engineering

SPIEDigitalLibrary.org/oe

Optical fiber sensors embedded in concrete for measurement of temperature in a real fire test

Antonio Bueno
Benjamín Torres
David Barrera
Pedro Antonio Calderón
José Manuel Lloris
María José López
Salvador Sales

SPIE

Optical fiber sensors embedded in concrete for measurement of temperature in a real fire test

Antonio Bueno
Universidad Politécnica de Valencia
iTEAM Research Institute
Optical and Quantum Communications Group
Camino de Vera s/n
46022 Valencia, Spain
E-mail: anbuemar@iteam.upv.es

Benjamín Torres
Universidad Politécnica de Valencia
Instituto de Ciencia y Tecnolgía del Hormigón ICITECH
Camino de Vera s/n
46022 Valencia, Spain

David Barrera
Universidad Politécnica de Valencia
iTEAM Research Institute
Optical and Quantum Communications Group
Camino de Vera s/n
46022 Valencia, Spain

Pedro Antonio Calderón
Universidad Politécnica de Valencia
Instituto de Ciencia y Tecnolgía del Hormigón ICITECH
Camino de Vera s/n
46022 Valencia, Spain

José Manuel Lloris
María José López
Instituto Tecnológico de la Construcción AIDICO
Avda. Benjamin Franklin 17
46980, Paterna, Valencia, Spain

Salvador Sales
Universidad Politécnica de Valencia
iTEAM Research Institute
Optical and Quantum Communications Group
Camino de Vera s/n
46022 Valencia, Spain

Abstract. We present the results of a real fire test using optical fiber sensors embedded in concrete samples. The temperature curve used in this experiment is described in the Spanish/European standard UNE-EN 1363-1 temperature profile for normalized concrete resistance to real fire tests, reaching temperatures of more than 1000°C inside the fire chamber and up to 600°C inside the concrete samples. Three types of optical sensors have been embedded in concrete: 1. standard fiber Bragg gratings inscribed in photosensitive germanium-boron co-doped fiber, 2. regenerated fiber Bragg grating (RFGB) inscribed in germanium doped fiber, and 3. RFBG inscribed in germanium-boron co-doped fiber. © *2011 Society of Photo-Optical Instrumentation Engineers (SPIE).* [DOI: 10.1117/1.3658760]

Subject terms: optical fiber temperature sensor; high temperature; fiber Bragg grating; regenerated fiber Bragg grating; fire test.

Paper 110921R received Aug. 3, 2011; revised manuscript received Oct. 4, 2011; accepted for publication Oct. 17, 2011; published online Nov. 18, 2011.

1 Introduction

The influence of fire on concrete structures has been reported in previous studies of structural damage because the strength of a concrete material decreases under the effect of high temperature.[1,2] To determine the damage produced by a fire to a concrete structure, some sensor elements need to be installed on the surface or inside the structure. Traditionally, electrical sensors have been used to obtain physical measurements of the structures, but recently some optical fiber sensors have been developed. Optical fiber sensors have the advantage that can be embedded in the concrete structures due to their small size.

In recent years optical fiber sensors for multiple applications have been widely used in the civil engineering field. Compared to the electrical sensors, the optical sensors present several advantages such as smaller and lighter, immunity to electromagnetic interference, (high temperature tolerance, and resistance to harsh environments. In addition, optical technology allows many sensors to be multiplexed in a single optical fiber in order to create a quasidistributed sensor system able to detect local damage.

0091-3286/2011/$25.00 © 2011 SPIE

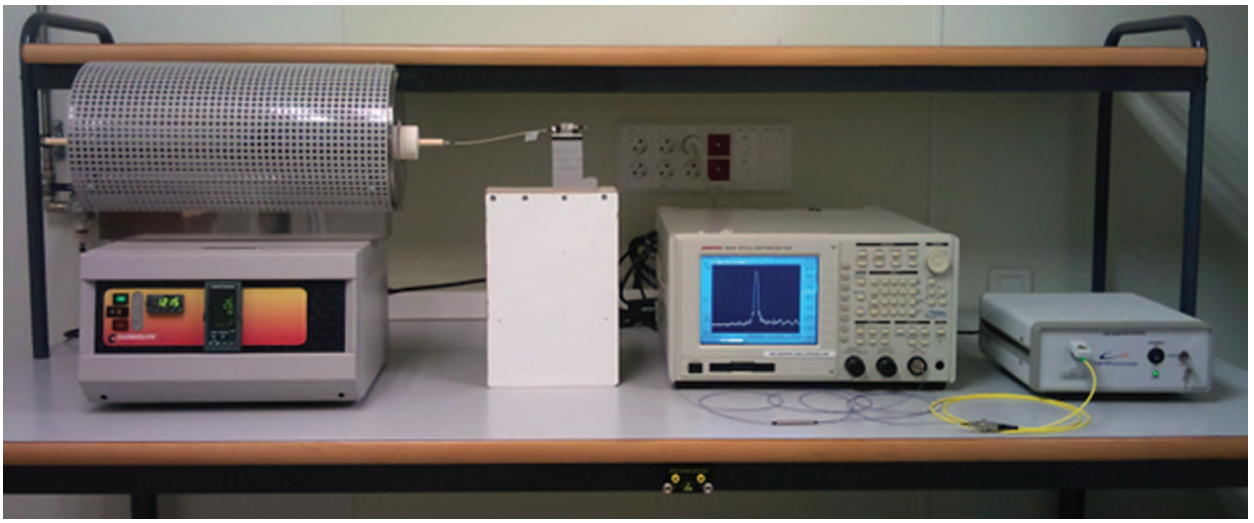

Fig. 1 Optical setup made for grating regeneration.

In this test, two concrete samples were placed in a fire chamber to perform a real fire test using embedded optical fiber temperature sensors. A normalized UNE-EN 1363-1 fire temperature curve was programmed into the fire chamber in order to obtain the heat transference inside the concrete samples. This real test is very helpful if the behavior of a concrete structure under fire is required, for example in a concrete tunnel, where the integrity of the structure has to be preserved in order to maintain the safety of the people inside the tunnel.

To date, previous publications concerning high temperature measurements in real structures using optical sensors have measured moderate high temperatures. In some works, embedded temperature sensors reached up to 150°C inside concrete specimens.[3,4] In another publication, external temperature sensors were employed to measure gas temperature, reaching a maximum temperature of 300°C.[5] Higher temperatures were measured in the experiments carried out by Heiberg et al.,[6] but in this case, embedding optical fiber Bragg grating (FBG) sensors and thermocouples into aluminum alloys. To the best of our knowledge, this is the first experiment of a real test fire of concrete structures with embedded optical fiber Bragg grating sensors.

In the present test, maximum temperatures up to 600°C inside the concrete beams are obtained corresponding to a chamber temperature close to 1100°C. Furthermore, three different types of optical temperature sensors, that will be described in Sec. 2, have been used in the test to compare their features at high temperature.

2 Sensors Development

All of the sensors used in this work are based on FBGs.[7] The gratings were created through the phase mask method using an UV beam at 244 nm from a frequency-double Argon laser. Up to four different phase masks were used to create gratings of central Bragg wavelengths at around 1529.4, 1534.2, 1539, and 1543.7 nm. The lengths of the gratings were set to 2 cm with an apodized profile of the refractive index to decrease the secondary lobes of the reflection spectrum and to improve the response of the sensors.

Three different types of optical sensors based on FBGs have been developed. The first type is a standard FBG and the other two sensors have been created by specifically treating a FBG in a two-step process. The first step in this process consists of the loading of hydrogen into an optical fiber[8] with 25 bars pressure for 15 days at room temperature. This hydrogen loaded fiber is then exposed to UV light to create the FBG, achieving the formation of hydroxyl groups in the core of the fiber. The second step in the creation of this type of sensor is the thermal treatment, which consists of a temperature ramp until the FBG is erased, then a steady state for several minutes in order to regenerate the grating and finally a cool down. The thermal annealing of the optical fiber leads to the creation of a much more stable FBG, being able to measure higher temperatures than a standard FBG. This new grating was first called chemical composition grating[9] due to the chemical processes present in the creation of the grating, but recently the new term of regenerated fiber Bragg grating (RFBG) is used,[10] referring to the regeneration process of the grating during the thermal step.

Depending on the initial FBG (also known as "seed"), the resulting RFBG has different properties. Two different types of optical fibers were used in the grating inscription. The first one was a standard germanium (Ge) doped optical fiber and the other one was a germanium and boron (Ge/B) co-doped photosensitive optical fiber. The main differences between them are the grating regeneration temperature (approximately 950°C in the Ge optical fiber and 550°C in the Ge/B optical fiber approximately) and the maximum

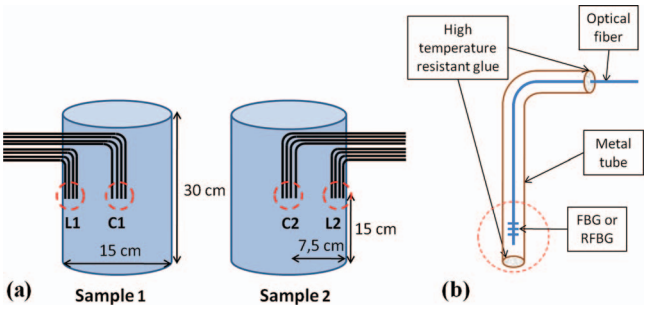

Fig. 2 (a) Sensor locations inside the concrete samples. (b) Detailed view of the sensor package.

Fig. 3 (a) Two sets of sensors fabricated. (b) Location of these sets inside the cylindrical mold before concrete pouring.

working temperature (1200°C in the Ge fiber and around 800°C in the Ge/B fiber). These thermal characteristics extend the temperature working limits of a standard FBG, established at a maximum temperature of 600°C. Besides, a standard FBG suffers from a highly significant reduction of the reflectivity when the temperature exceeds 300°C. Figure 1 shows the setup made for the thermal treatment in order to achieve the grating regeneration. A tubular oven was used to heat the grating and an optical broadband source and an optical spectrum analyzer were used to monitor the grating's reflectivity.

Once the FBGs and RFBGs were created, it was necessary to develop a suitable protection to prevent damage to the optical fiber during the installation of the sensors. A simple sensor head was fabricated by introducing the optical fiber (containing an FBG or an RFBG) inside a hollow metal tube sealed at both ends. A good seal is helpful in the sensor transportation and it also prevents the accidental introduction of fresh concrete inside the tube during the installation. Therefore the ends of the metal tube were sealed with high temperature resistant glue. As a result, the fiber remains loose inside the tube and is kept away from any external agent and is free from the strain applied to the tube [Fig. 2(b)].

Electrical sensors were also placed, consisting of thermocouples type K able to measure temperatures up to 1000°C. These sensors were used to compare the measurements between optical and electrical sensors.

As a result of this process, four sets of sensors were fabricated, each one of them containing:

- 1 standard FBG sensor inscribed in a photosensitive Ge/B co-doped optical fiber.
- 1 RFBG sensor inscribed in a Ge doped optical fiber.
- 1 RFBG sensor inscribed in a photosensitive Ge/B co-doped fiber.
- 1 type K electrical thermocouple.

Table 1 Sensors installed inside the concrete samples.

Specimen	Location	Sensors installed
Sample 1	L1	Ge#1, Ge/B#1, FBG#1, TC#1
	C1	Ge#2, Ge/B#2, FBG#2, TC#2
Sample 2	L2	Ge#3, Ge/B#3, FBG#3, TC#3
	C2	Ge#4, Ge/B#4, FBG#4, TC#4

3 Installation of Sensors and Concrete Samples

The fabricated sets of sensors mentioned in Sec. 2 were installed inside two concrete samples. These samples were made in a cylindrical shape, having a size of 30 cm height and 15 cm diameter. Two sets of sensors were embedded in each concrete specimen in two specific locations: the lateral side and the center of gravity (7.5 cm from the lateral side and 15 cm height). Figure 2(a) shows the schematic locations of the sensors in points L1 (lateral side) and C1 (center of gravity) in sample 1 and L2 (lateral side) and C2 (center of gravity) in sample 2.

The sensors were labeled as FBG#1..4 for the FBG sensors, Ge#1..4 for the RFBG inscribed in Ge-doped fiber, Ge/B#1..4 for the RFBG inscribed in Ge/B co-doped fiber, and TC#1..4 for the thermocouples. It can be seen in Table 1 the locations of every single sensor inside the concrete samples after the installation. The sets of sensors were fixed to two cylindrical molds, and then the concrete was carefully poured into each of them, completely covering the sensing heads of the sensors. Figure 3 shows two sets of sensors fabricated on the left, and the location of these sets inside the cylindrical mold before the concrete pouring, on the right. The concrete samples were removed from their molds after 48 h, when the concrete had reached almost 80% of its final strength. The next step was to move the samples to a specific

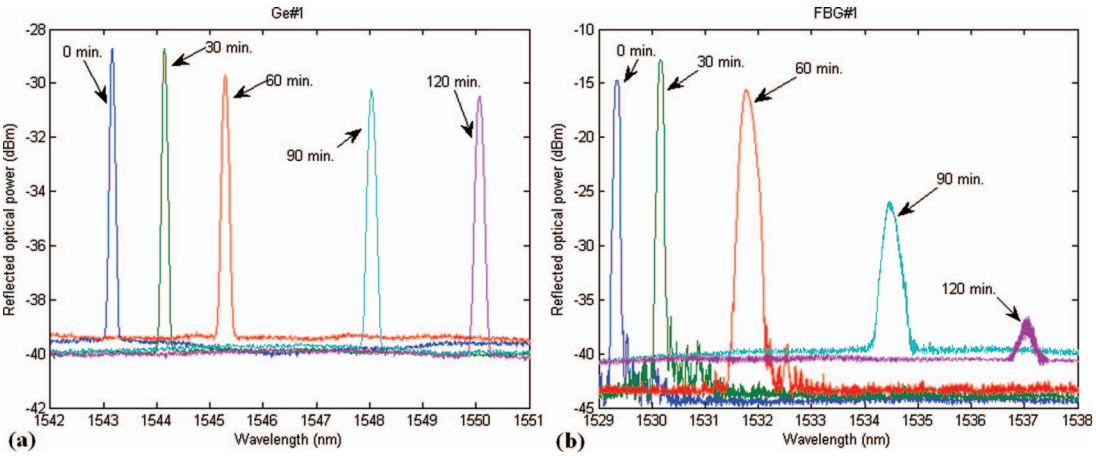

Fig. 4 Spectrum evolution at different times during the test of sensors: (a) Ge#1 and (b) FBG#1.

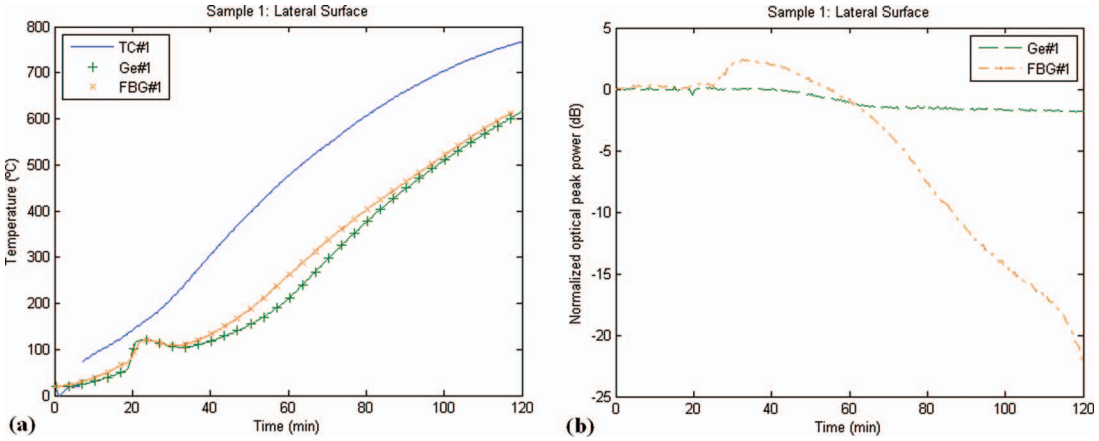

Fig. 5 Sample 1 at lateral surface (point L1): (a) Temperature measured by optical and electrical sensors and (b) normalized optical peak power of the optical sensors.

concrete cure chamber where the samples were held for 34 days until they reached their maximum strength.

The two concrete samples were moved to a fire chamber to perform the temperature test. The size of the fire chamber was 1.5 m × 1.5 m × 1.5 m, containing four burners that were capable of increasing the temperature inside the chamber to above 1200°C. The burners were monitored by four different electrical thermocouples located inside the chamber. The concrete samples were positioned at the lateral sides of the floor inside the chamber. The metal tubes containing the sensors were extended about 30 cm and fed out of the fire chamber through a 2 cm diameter hole in order to allow the optical connections to the measurement equipment outside the chamber. A commercially available sensor interrogator was used to collect the data from the optical sensors during the test.

After the installation of the concrete samples, the sensor named Ge/B#1 appeared to be broken due to the transportation of the concrete specimens. Thus, the survival percentage during installation concerning the optical sensors was 93.75%.

4 Real Fire Temperature Test

The Spanish/European standard UNE-EN 1363-1 temperature profile for normalized concrete resistance to real fire was used. The formula used for the temperature increment is:

$$\Delta T = 345 \log(8t + 1), \tag{1}$$

where t is time in minutes. According to Eq. (1), the target increment of temperature has a very fast initial response, followed by a slower temperature rise. The duration of the test was 120 min, when the temperature measured by the thermocouples inside the chamber was around 1060°C.

The data obtained by the optical sensor interrogator was converted to temperature by applying a second order temperature sensitivity of 8.6 pm/K and 7.97×10^{-3} pm/(K^2) to the sensors inscribed in germanium-boron co-doped fiber and 11.79 pm/K and 2.45×10^{-3} pm/(K^2) to the sensors inscribed in germanium doped fiber. Sensitivity factors of the optical sensors were previously obtained through a calibration test. The spectrum of the gratings was also recorded in order to monitor the variation of the reflectivity with temperature. In addition, the shape of the grating's spectrum changes. Indeed, it can be observed in Fig. 4(b) that the peak power reflected by FBG#1 decreases more than 20 dB and its spectrum become broader. On the other hand, the spectrum of RFBG Ge#1 remains almost unchanged [Fig. 4(a)].

Figures 5(a)–8(a) show the temperature evolution and Figs. 5(b)–8(b) show the normalized peak power reflected

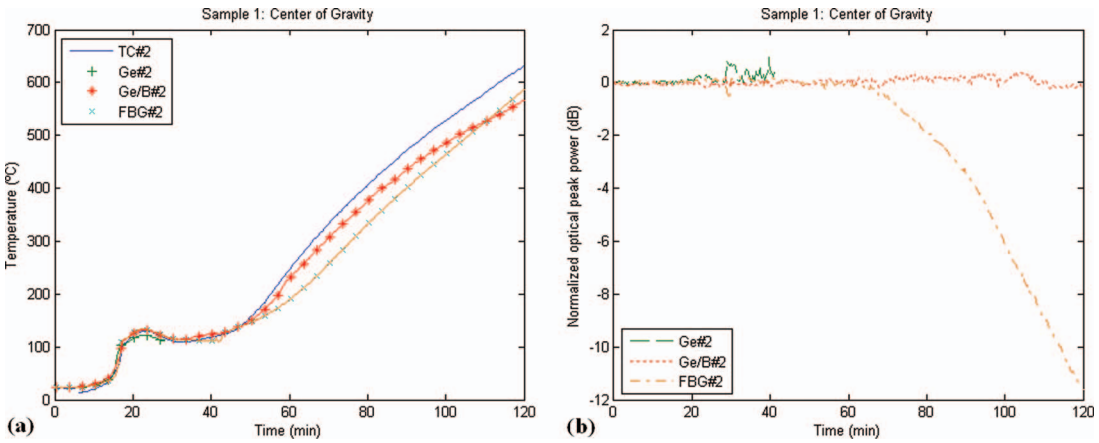

Fig. 6 Sample 1 at the center of gravity (point C1): (a) Temperature measured by optical and electrical sensors and (b) normalized optical peak power of the optical sensors.

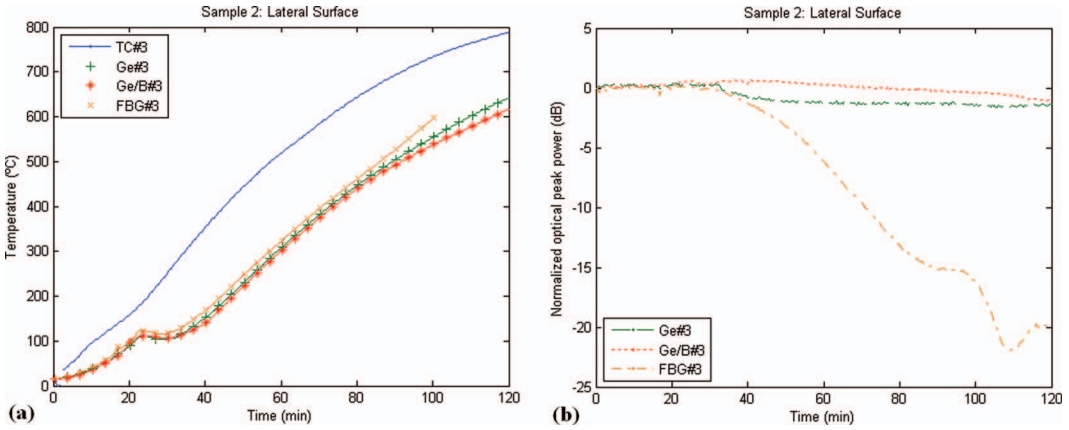

Fig. 7 Sample 2 at the lateral surface (point L2): (a) Temperature measured by optical and electrical sensors and (b) normalized optical peak power of the optical sensors.

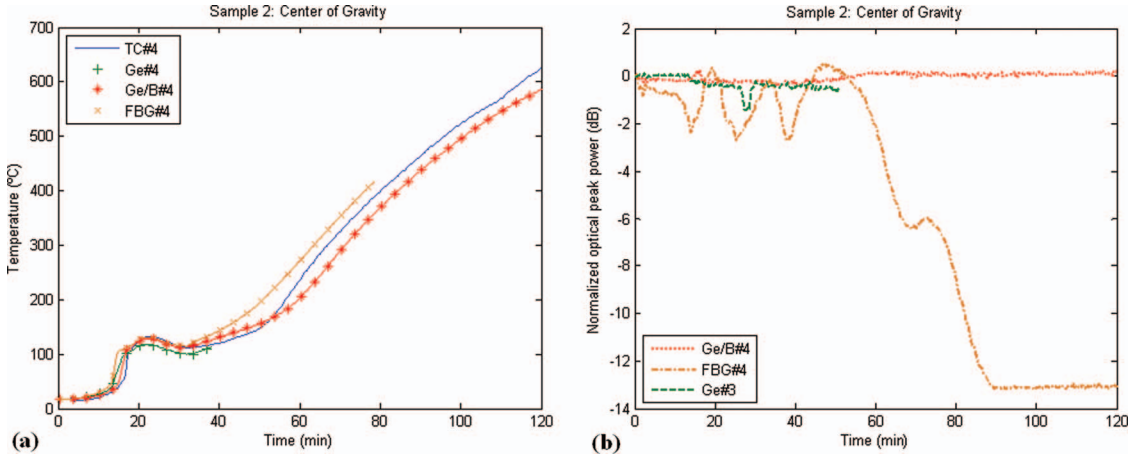

Fig. 8 Sample 2 at the center of gravity (point C2): (a) Temperature measured by optical and electrical sensors and (b) normalized optical peak power of the optical sensors.

Table 2 Maximum temperatures measured by optical and electrical sensors.

	Sample 1		Sample 2	
	#1 (L1)	#2 (C1)	#3 (L2)	#4 (C2)
Ge	615.3°C	Spectrum disappearance	641.7°C	Spectrum disappearance
Ge/B	not available	566.5°C	617°C	586.3°C
FBG	613.9°C	587.4°C	Erased at around 100 min	Erased at around 80 min
Thermocouple	767°C	631°C	788°C	625°C

Table 3 Optical power losses of optical sensors after the test.

	Sample 1		Sample 2	
	#1 (L1)	#2 (C1)	#3 (L2)	#4 (C2)
Ge	1.83 dB	Spectrum dissapearance	1.4 dB	Spectrum dissapearance
Ge/B	not available	0.11 dB	1.01 dB	0.1 dB
FBG	22.46 dB	more than	more than	more than
		11.55 dB	19.86 dB	13.03 dB

by the gratings during the fire test. It can be seen that at the center of gravity of both concrete samples (points C1 and C2) the temperature measured by the thermocouples and the optical sensors is very similar, whereas the temperature profile is rather different on the lateral surface (points L1 and L2). This is due to the location of the sensors during the installation and the temperature gradient inside the concrete sample. The thermocouples were the nearest sensors to the lateral side in both concrete samples, thus inside the chamber they were more exposed to the fire created by the burners. In addition, the temperature gradient is higher at the air-concrete interface during the heating process,[1] and the thermocouples were also installed very close to that interface.

Figures 5(a)–8(a) also show a temperature ramp registered by the optical sensors at around 20 min. This is due to the thermal inertia of concrete[11] which consists of a time delay in the transference of heat through the concrete mass when the temperature changes from room temperature (∼22°C) to a temperature higher than 500°C in only 5 min.

Concerning sample 1 at point L1 (Fig. 5), the maximum temperature registered by FBG#1 was 613.9°C, although its reflectivity decreased 22.46 dB after 118 min from the start of the test, thus the Bragg wavelength was not clearly identified by the peak search algorithm used. At the same location, Ge#1 shows a maximum temperature of 615.3°C after 120 min with only losses of 1.83 dB. The thermocouple TC#1 located at this point shows a maximum temperature of 767°C.

Taking a look at point C1 in sample 1 (Fig. 6), a similar behavior can be seen in every sensor located at this point. Unfortunately, sensor Ge#2 disappeared after 42 min. This is due to light reflections at the fiber splice since the noise floor increased above the reflected peak power of the grating, meaning that the peak search algorithm was unable to follow the wavelength shift. The Ge/B#2 sensor registered a maximum temperature of 566.5°C and FBG#2 registered 587.4°C. Thermocouple TC#2 showed a maximum temperature of 631°C. Concerning optical losses, Ge/B#2 had only losses of 0.11 dB whereas FBG#2 had losses of 11.55 dB.

Moving onto sample 2 at point L2 (Fig. 7), the maximum temperatures measured by the optical sensors were: 641.7°C by Ge#3, 617°C by Ge/B#3, and 598.2°C by FBG#3 (although this sensor disappeared after 100 min), whereas termocoupler TC#3 measured a maximum temperature of 788°C. Optical losses experienced by the optical sensors were: 1.4 dB by Ge#3 sensor, 1.01 dB by Ge/B#3 sensor, and more than 19.86 dB by FBG#3 sensor.

At point C2 in sample 2 (Fig. 8), the results were similar to those obtained at point C1 in sample 1. The Ge#4 sensor disappeared at an early stage, after 52 min. This is again due to the problems originated in the splice. The maximum temperatures registered by the rest of the optical sensors were: 586.3°C by Ge/B#4 sensor and 417.9°C by FBG#4 sensor (although its optical peak power disappeared in minute 79 due to the high losses). Thermocouple TC#4 measured a maximum temperature of 625°C. Optical losses experienced by the optical sensors were: 0.1 dB by Ge/B#4 sensor and 13.03 dB by FBG#4 sensor.

All the results extracted from this test are summarized in Table 2 concerning maximum temperature registered by the optical and electrical sensors and in Table 3 concerning the optical power losses in the peak power reflected by the gratings at the end of the test, normalized by the reflected peak power at the beginning of the test.

5 Conclusions

The optical sensors show a good agreement with the electrical ones at the center of gravity of both concrete samples. In the lateral surfaces there are some differences between the measurements obtained from the sensors located at this point. This is due to the position of the sensors during the installation and the temperature gradient inside the concrete sample. To be precise, the thermocouples were installed very close to the air-concrete interface, where the temperature gradient is higher. The optical sensor registered temperatures above 600°C inside the concrete specimens whereas the temperature inside the chamber was around 1060°C after 120 min.

The standard FBG sensors were completely erased during the test due to the high temperature, resulting in a decrease in the reflected peak power of the grating until the noise floor. Nevertheless, FBG sensors can be used in high temperature tests if the time duration of the experiment is short enough, and they can be reusable in a high temperature environment if the reflectivity losses of the grating during the previous tests are small enough.

The Ge and Ge/B doped fiber RFBG sensors have shown much less optical losses. However, the process of the fabrication of the RFBG is more complex. Thus, for each application one or the other type of optical sensor can be chosen. In our case, RFBG sensors appear to be useful sensors for high temperature applications, such as fire detection inside a tunnel, as they can withstand temperatures over 1000°C (Ref. 10) and the fire can be detected when the temperature extremely rises in the first minutes.

Acknowledgments

The authors gratefully acknowledge research funding by the Spanish Ministry of Science and Innovation through Project SOPROMAC P41/08.

References

1. B. M. Luccioni, M. I. Figueroa, and R. F. Danesi, "Thermo-mechanic model for concrete exposed to elevated temperatures," *Eng. Struct.* **25**, 729–742 (2003).
2. H. Abdel-Fattah and S. A. Hamoush, "Variation of the fracture toughness of concrete with temperature," *Constr. Build. Mater.* **11**(2), 105–108 (1997).
3. J. C. Cardozo da Silva, C. Martelli, H. J. Kalinowsky, E. Penner, J. Canning, and N. Groothoff, "Dynamic analysis and temperature measurements of concrete cantilever beam using fibre Bragg gratings," *Opt. Lasers Eng.* **45**, 88–92 (2007).
4. Y. B. Lin, J. C. Chern, K. C. Chang, Y. W. Chan, and L. A. Wang, "The utilization of fiber Bragg grating sensors to monitor high performance concrete at elevated temperature," *Smart Mater. Struct.* **13**, 784–790 (2004).
5. A. Lönnermark, P. O. Hedekvist, and H. Ingason, "Gas temperature measurements using fibre Bragg grating during fire experiments in a tunnel," *Fire Saf. J.* **43**, 119–126 (2008).
6. G. Heiberg, J. Skaar, M. Fokine, and L. Arnberg, "A new method for temperature measurement in solidifying aluminum alloys by use of optical fiber Bragg grating sensors," Proc. of 106th American Foundry Society Casting Congress, Kansas, MO, *Trans. Am. Foundry Soc.* **110**, Part 1, 383–391 (2002).
7. A. D. Kersey, M. A. Davis, H. J. Patrick, M. LeBlanc, K. P. Koo, C. G. Askins, M. A. Putnam, and E. J. Friebele, "Fiber grating sensors," *J. Lightwave Technol.* **15**(8), 1442–1463 (1997).
8. C. L. Liou, L. A. Wang, and M. C. Shih, "Characteristics of hydrogenated fiber Bragg gratings," *Appl. Phys. A* **64**, 191–197 (1997).
9. M. Fokine, "Underlying mechanisms, applications, and limitations of chemical composition gratings in silica based fibers," *J. Noncrystalline Solids* **349**, 98–104 (2004).
10. S. Bandyopadhyay, J. Canning, M. Stevenson, and K. Cook, "Ultrahigh-temperature regenerated gratings in boron-codoped germanosilicate optical fiber using 193 nm," *Opt. Lett.* **33**, 1917–1919 (2008).
11. L. Ropelewski and R. D. Neufeld, "Thermal inertia properties of autoclaved aerated concrete," *J. Energy Eng.* **125**(2), 59–75 (1999).

Antonio Bueno received a BSc degree in telecommunications in 2008 and an MSc degree in technologies, systems and networks of communication in 2010, both from the Universidad Politécnica de Valencia (UPV), Spain. He is currently working toward his PhD in optics at the Universidad Politécnica de Valencia in the Optical and Quantum Communications Group at iTEAM research institute under the supervision of Dr. Salvador Sales. His fields of interest are fiber Bragg grating and Brillouin fiber sensors.

Benjamín Torres received his BSc degree in civil engineering in 2008 and his MSc degree in concrete engineering in 2009, both from the UPV, Spain. He is currently working toward his PhD in civil engineering at the Universidad Politécnica de Valencia in the Concrete Science and Technology Research Group (ICITECH) under the supervision of Dr. Pedro A. Calderón. His fields of interest are fiber optic sensors for structural health monitoring, forensic engineering, and structural repairs.

David Barrera received his MSc degree in telecommunications engineering from the UPV in 2006. Since then, he has been working at the Optical and Quantum Communications Group of the iTEAM research institute. His research interests include fiber Bragg grating, optical fiber sensing, and polymer optical fibers. He is currently working toward his PhD degree at the Universidad Politécnica de Valencia and focusing on optical fiber sensing.

Pedro Antonio Calderón is a professor in the Department of Civil Engineering of Universidad Politécnica de Valencia (Spain) since 1999. He obtained his BSc degree in civil engineering at the UPV in 1986, an MSc degree in geotechnical engineering at the University of California, Davis, in 1990, and his PhD at the UPV in 1992. He has been the director of the technical department of the company GIA (mainly dedicated to structural and geotechnical monitoring and assessment) from 1991 to 1999. He is currently the director of the building structures research group at the ICITECH, where he is currently involved in the topic “structural health monitoring.” He is the author of more than 50 international papers and communications.

José Manuel Lloris has a PhD in chemistry from the Universidad Politécnica de Valencia in 2000 working toward the development of new electrochemical sensors. Since 2005 he is a senior researcher in the Materials Research Unit of AIDICO, Technological Research Center for Construction Materials. His work is focused on the nanomateriales area, synthesis of nanoparticles, functional materials, and smart systems. He has experience in the development of new materials with more than 40 papers. From 2001 to 2004 he gained a post-doctoral stage in the University of Cordoba. He worked on solid state chemistry to develop new lithium and sodium insertion materials.

María José López: biography not available.

Salvador Sales is a professor in the Departamento de Comunicaciones, Universidad Politécnica de Valencia, Spain. He is also working in the iTEAM research institute. He received MSc and PhD degrees in telecomunicación from the Universidad Politécnica de Valencia. He is currently the coordinator of some Ph D telecomunicación students at Universidad Politécnica de Valencia. He is the co-author of more than 60 journal papers and 100 international conferences. He has been collaborating and leading some national and European research projects since 1997. His main research interests include fiber Bragg gratings, WDM and Subcarrier Multiplexing (SCM) lightwave systems, and semiconductor optical amplifiers.